Precisely locating the Ordovician equator in Laurentia

Jisuo Jin[1]*, David A. T. Harper[2], L. Robin M. Cocks[3], Phil J. A. McCausland[1], Christian M. Ø. Rasmussen[4], Peter M. Sheehan[5]

[1]*Department of Earth Sciences, Western University, London, Ontario N6A 5B7, Canada*

[2] *Department of Earth Sciences, Durham University, Durham DH1 3LH, UK*

[3] *Department of Earth Sciences, The Natural History Museum, London SW7 5BD, UK*

[4] *Natural History Museum, University of Copenhagen, Copenhagen K-1350, Denmark*

[5] *Department of Geology, Milwaukee Public Museum, Milwaukee, Wisconsin 53233, USA*

GSA Data Repository Item 2013026, includes supplementary introduction and methods, five supplementary figures (DR 1 to DR5) and one supplementary table (Table DR1).

Introduction and Methods

The hurricane-free equatorial zone today and the recognition Late Ordovician equatorial biofacies

The formation of hurricanes, or cylogenesis, requires the convergence of several physical parameters. Among the six commonly cited meteorological conditions (Gray, 1981), the key parameters include a sufficiently strong Coriolis force (usually >10° north and south of the equator) and high sea surface temperatures (usually >26°C) to generate large amount of unstable thunderclouds moving with the rising branch of the Hadley cell of atmospheric circulation. In the northern hemisphere, for example, the probability of hurricane formation increases during the summer when the intertropical convergence zone (ITCZ; also known as the doldrums) shifts northwards from the equator. The global record of named hurricanes (1842-2009) compiled from the database of the National Hurricane Center of the National Oceanic and Atmospheric Administration (NOAA, 2011, http://www.csc.noaa.gov/hurricanes/#) clearly shows that category 1 to 5 hurricanes/cyclones usually do not occur within 10 degrees north and south of the equator, mainly because the Coriolis force is too weak near the equator (Fig. DR1). This hurricane-free zone, however, may or may not coincide with the ITCZ because the former is controlled mainly by the Coriolis force, whereas the latter shifts with the azimuth of the sun. Despite the hurricane-free equatorial zone being a well-known oceanographic feature today, there has been little study dealing with the Paleozoic sedimentological and paleobiological records associated with this special environment. In this study, we provide the first case study of identifying Paleozoic biofacies that are indicative of paleoequatorial hurricane-free depositional settings, based on the following working hypotheses:

1) Comparison of modern and Paleozoic hurricane patterns has been strengthened by recent studies showing that cold south polar regions with permanent ice caps probably existed during the Late Ordovician and Early Silurian (Finnegan et al., 2011). Thus it is reasonable to assume that Late Ordovician temperature gradient between the polar and tropical areas, and hence the hurricane pattern, was analogous to that on Earth today.

2) Strong hurricanes or cyclones, usually in the tropics between 10–30° latitudes, are capable of generating long-period waves that can disturb and rework sediments up to 120 m or deeper.

3) A suite of sedimentary features is known to be generated by hurricane-grade storms, such as hummocky cross stratification (HCS) that forms between fair-weather wave base and maximum storm wave base, usually 15–120 m (Dumas and Arnott, 2006). Shell-bearing sediments below fair-weather wave base can be suspended and redeposited by severe storms as amalgamated shell coquinas and segregated mud drapes, often with prominent scoured bases, HCS, and graded bedding (Kidwell, 1985).

4) In the rock record, tropical biofacies may be an indicator of the hurricane-free equatorial zone if they are typical of shallow open marine environments (i.e. within the depth range hurricane disturbance) but did not show severe storm-generated sedimentary structures.

The *Proconchidium* brachiopod shell beds from North Greenland (Figs. DR2, DR3) discussed in this paper are examples of the biofacies without hurricane disturbance, although the G.B. Schley Fjord locality corresponds to a shallow-water (within photic zone), open continental shelf environment in the northeastern margin of Laurentia. This type of non-amalgamated brachiopod shell beds (NABS) accumulated in a somewhat shallow-water depositional environment than the massive-bedded *Thalassinoides* facies (MBTF), near the fair-weather wave base. In addition to the sedimentological evidence discussed in the main text, the *Thalassinoides* beds intercalated with the NABS at the Schley Fjord section are notably thinner and irregular in comparison to the typical MBTF, due to the influence of fair-weather waves (see Fig. 2E).

In contrast to the *Proconchidium* NABS of North Greenland, the *Virgiana* shell beds, composed of brachiopod shells of similar size and shape as, and of close phylogenetic relationship to, *Proconchidium*, are found in a comparable shallow-water, open-marine shelf environment of Anticosti Island (locality 13, Fig. 1), but have striking sedimentary structures generated by severe storms (Fig. 3; Fig. DR4).

In this study, the two types of paleobiological indicators: massive-bedded *Thalassinoides* facies (MBTF) and non-amalgamated brachiopod shell beds (NABS), agree well with the paleomagnetic data in locating the Late Ordovician equator. In high paleotropical latitudes (e.g. localities 10–13, Fig. 1), these biofacies disappear and are replaced by carbonate rocks with common sedimentary structures (HSC, scours and channels, graded bedding, amalgamated coquinas or bioclastic grainstones) generated by severe storms in relatively deep water (15–100 m), such as those in the Upper Ordovician strata of southern Ontario, western New York State (Brookfield and Brett, 1988), Pennsylvania (Duke, 1987); Ohio (Ettensohn et al., 2002), and Anticosti Island, Quebec (Long, 2007).

Below is a list of the various paleobiological localities (with key references) used for analysis of paleolatitudical gradient (Fig. 1):

1, Børglum Elv, North Greenland; 2, Schley Fjord, North Greenland; 3, Brodeur Peninsula, Baffin Island; 4, southern Manitoba; 5, Bighorn Mountain, northern Wyoming (Holland and Patzkowsky, 2007); 6–9, border area of Utah-Nevada, Great Basin (Sheehan and Schiefelbein, 1984); 10, Cincinnati type areas, Ohio-Kentucky-Indiana tri-state borderland; 11, Lake Simcoe area, Ontario; 12, Trenton area, New York State; 13, Anticosti Island, Quebec.

Determining the Ordovician south pole using paleobiological and paleomagnetic data

The following localities have been used to determine the Late Ordovician south pole position for Laurentia (-13.5EN, 326.5 E; A95=13.5E) by assuming that each locality was located at the paleoequator and then solving for the best for intersection of great circles to each locality (see Fig. DR5). Faunal localities are given in present North American coordinates. Localities in North Greenland have been rotated to present North America coordinates using the Euler rotation 67.5 EN, -118.5 E, angle -14E to correct for Mesozoic-Cenozoic rifting.

Massive-bedded *Thalassinoides* facies (MBTF; see Table DR1)

1, Gillis Quarry, Garson, southern Manitoba, 50°04’30”N, 96°41’45”W.

2, Hunt Mountain, Bighorn Mountains, Wyoming (Holland and Patzkowsky, 2007), 44°44’19.4”N, 107°43’41.3”W.

3, Børglum Elv, Peary Land, North Greenland, 82°28’29.7”N, 30°45’22.8”W.

4, Great Basin, Nevada and Utah, southwestern USA (Sheehan and Schiefelbein, 1984). **A**, Barn Hills, Utah. 38°58’36”N, 113°23’25”W. **B**, Tony Grove Lake, Utah, 41°53’30.5”N, 111°38’51.8”W. **C**, Tony Grove Lake, Utah, 41°53’30.5”N, 111°38’51.8”W. **D**, Toano Range, Nevada, 41°2’5”N, 114°15’12”W. **E**, Ricks Canyon, Newfoundland Range, Utah, 41°8’37”N, 113°22’39”W. **F**, Lakeside Mountains, Utah, 40°52’25”N, 112°45’28”W.

Non-amalgamated brachiopod shell beds (NABS; see Table DR1)

1, G.B. Schley Fjord, Peary Land, North Greenland, 82°54’56.8”N, 25°44’56.7”W.

2, northeastern Brodeur Peninsula, Baffin Island, 73°33’02”N, 85°22’00”W.

References

Brookfield, M.E. and Brett, C.E., 1988. Paleoenvironments of the Mid-Ordovician (Upper Caradocian) Trenton limestones of southern Ontario, Canada: Storm sedimentation on a shoal-basin shelf model. Sedimentary Geology, v. 57, p. 75–105.

Duke, W.L., 1987. Reply, Hummocky cross-stratification, tropical hurricanes, and intense winter storms. Sedimentology, v. 34, p. 344–359.

Dumas, S. and Arnott, R.W.C., 2006. Origin of hummocky and swaley cross-stratification – The controlling influence of unidirectional current strength and aggradation rate. Geology, v. 34, p. 1073–1076.

Ettensohn, F.R., Kulp, M.A. and Rast, N., 2002. Interpreting ancient marine seismites and apparent epicentral areas for paleo-earthquakes, Middle Ordovician Lexington Limestone, central Kentucky. Geological Society of America Special Paper, v. 359, p. 177–190.

Finnegan S. et al., 2011. The magnitude and duration of Late Ordovician–Early Silurian glaciation. Science, v. 331, p. 903–906.

Gray, W.M., 1981. Recent Advances in Tropical Cyclone Research from Rawinsonde Composite Analysis. World Meteorological Organization.

Holland, S.M. and Patzkowsky, M.E., 2007. Gradient ecology of a biotic invasion: biofacies of the type Cincinnatian Series (Upper Ordovician), Cincinnati, Ohio region, USA. Palaios, v. 22, p. 392–407.

Kidwell, S.M., 1985. Palaeobiological and sedimentological implications of fossil concentrations. Nature, v. 318, p. 457–460.

Long, D.G.F., 2007. Tempestite frequency curves: a key to Late Ordovician and Early Silurian subsidence, sea-level change, and orbital forcing in the Anticosti foreland basin, Quebec, Canada. Canadian Journal of Earth Sciences, v. 44, p. 413–431.

Sheehan, P.M. and Schiefelbein, D.R.J. 1984. The trace fossil *Thalassinoides* from the Upper Ordovician of the eastern Great Basin: deep burrowing in the Early Paleozoic. Journal of Palaeontology, v. 58, p. 440–447.

Supplementary Figures

Figure DR1. Global occurrences of named tropical storms and hurricanes (1842-2009) compiled by the National Hurricane Center of the National Oceanic and Atmospheric Administration (http://www.csc.noaa.gov/hurricanes/#). Hurricane categories based on maximum sustained wind (MSW): category 5 (H5) >249 km/hr; H4, 210-249 km/hr; H3, 178-209 km/hr; H2, 154-177 km/hr; H1, 119-153 km/hr; tropical storm (TS), 62-118 km/hr; tropical depression (TD), <62 km/hr.

Figure DR2. Stratigaphical log of the Upper Ordovician section in G.B. Schley Fjord, Peary Land, North Greenland. Recurrences of non-amalgamated brachiopod shell beds (NABS) represent a temporally stable depositional environment associated with a combination of two conditions – shallow, open marine water (indicated by the presence of receptaculitid *Fisherites* and large stromatoporoid sponges and that were either photoautotrophic of photosymbion-bearing), but a substrate lacking disturbances by severe storms.

Figure DR3. *Proconchidium* shell beds, example of the non-amalgamated brachiopod shell beds (NABS), Lower Turesø Formation (upper Katian), Schley Fjord, Peary land, eastern North Greenland. Individual shell beds have a thickness up to 1 m (= tape measure) and are dominated by largely in-situ, extremely thickened ventral valves that are randomly distributed in undisturbed carbonate mud (B, C). Note lack of hummocky cross stratification (HCS) or other sedimentary structures generated by severe storms.

Figure DR4. A: *Virgiana* shell beds, lower Becscie Formation (Rhuddanian, basal Silurian), Anticosti Island, eastern Canada. Note pervasive hummocky cross stratification (HSC), scoured and channelled base, and segregation/amalgamation of shells from draping mud (B), all typical structures generated by hurricane-grade storms in contrast to non-amalgamated shell beds (C) shown in Fig. 3.

Figure DR5. Comparison of Late Ordovician south pole positions (SSP) determined independently from paleobiological and paleomagnetic data. A: "Paleobiological SSP" is derived from biofacies localities (Table DR1) based on the best pole solution with a 95% cone of confidence radius of 13.5° for intersecting 90° great circles to each of the faunal localities in the Great Basin, southern Manitoba, and North Greenland. Paleomagnetic results from the coeval Juniata Formation red beds (26° ± 12° paleolatitude at sampling locality) provide a swathe of permissible Late Ordovician SSP (thick dashed line). B: Apparent Polar Wander Path (APWP) for the Early Paleozoic of Laurentia, plotted as south poles from 532 Ma to 420 Ma. Cambrian poles are shown with dotted 95% confidence ellipses; Ordovician and Silurian poles are shown with solid 95% confidence ellipses. Globes for A and B are presented in present-day North American coordinates as an orthogonal projection centered at 15°N, 330 E. Abbreviations are given in Table DR1.

Supplementary Table

Table DR1. Paleobiological and paleomagnetic data used for determining the Late Ordovician south pole positions (SSP) as shown in Fig. DR5. Unit age is given as a chronostratigraphic age with numerical age inferred (in Ma); Location is the central latitude and East longitude of the paleomagnetic study sites. N: Number of paleomagnetic sites in a given study which define its result. Paleomagnetic result is the mean direction reported, with *D* = declination, *I*E = inclination, and *α95*E = the radius of the cone of 95% confidence about the direction. Paleopole (south): Calculated south pole position relative to Laurentia, with A95E representing the radius of 95% confidence about the pole position. *Q* = Quality value (maximum of 7); REFNO is the paleomagnetic result reference in the Global Paleomagnetic Database (ver. 4.6).

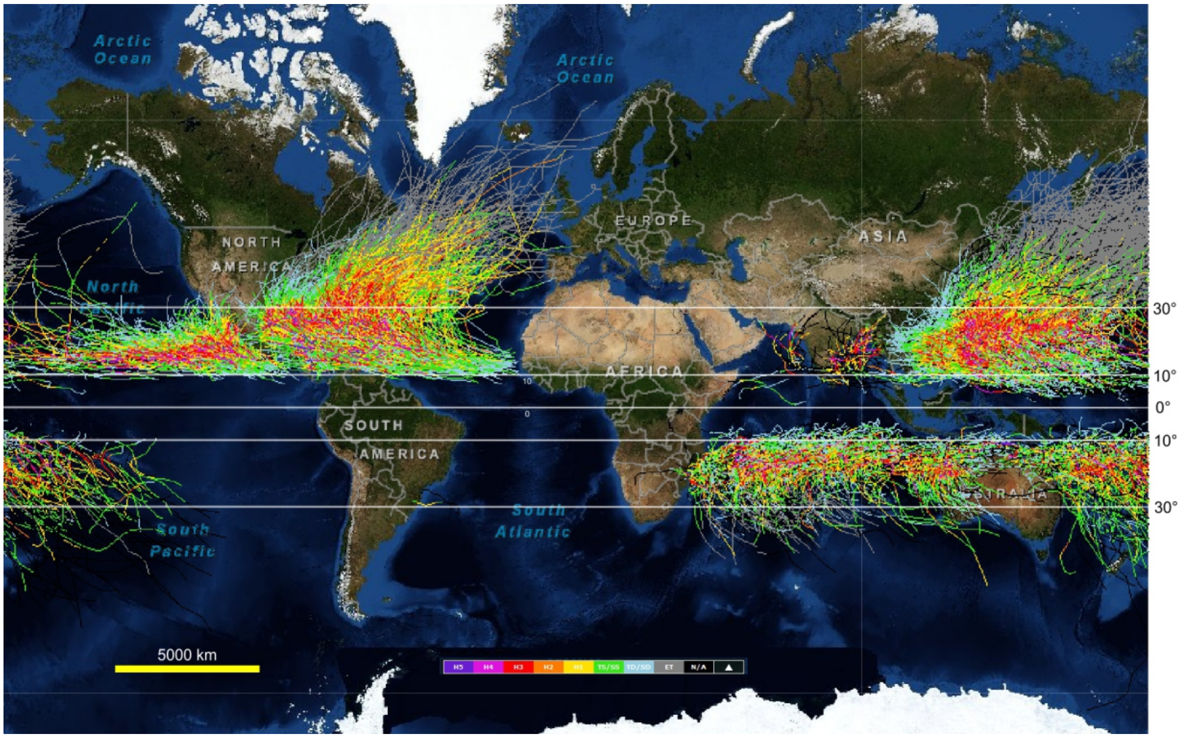

Fig. DR1. Global occurrences of named hurricanes and tropical storms from 1842 to 2009, compiled from the database of the National Hurricane Center, National Oceanic and Atmospheric Administration (NOAA, 2011,) of the United States of America (http://www.csc.noaa.gov/hurricanes/#). Hurricane categories are based on maximum sustained wind (MSW): Category 5 hurricane (H5) >249 km/hr; H4, 210-249 km/hr; H3, 178-209 km/hr; H2, 154-177 km/hr; H1, 119-153 km/hr; tropical Storm (TS), 62-118 km/hr; tropical depression (TD), <62 km/hr.

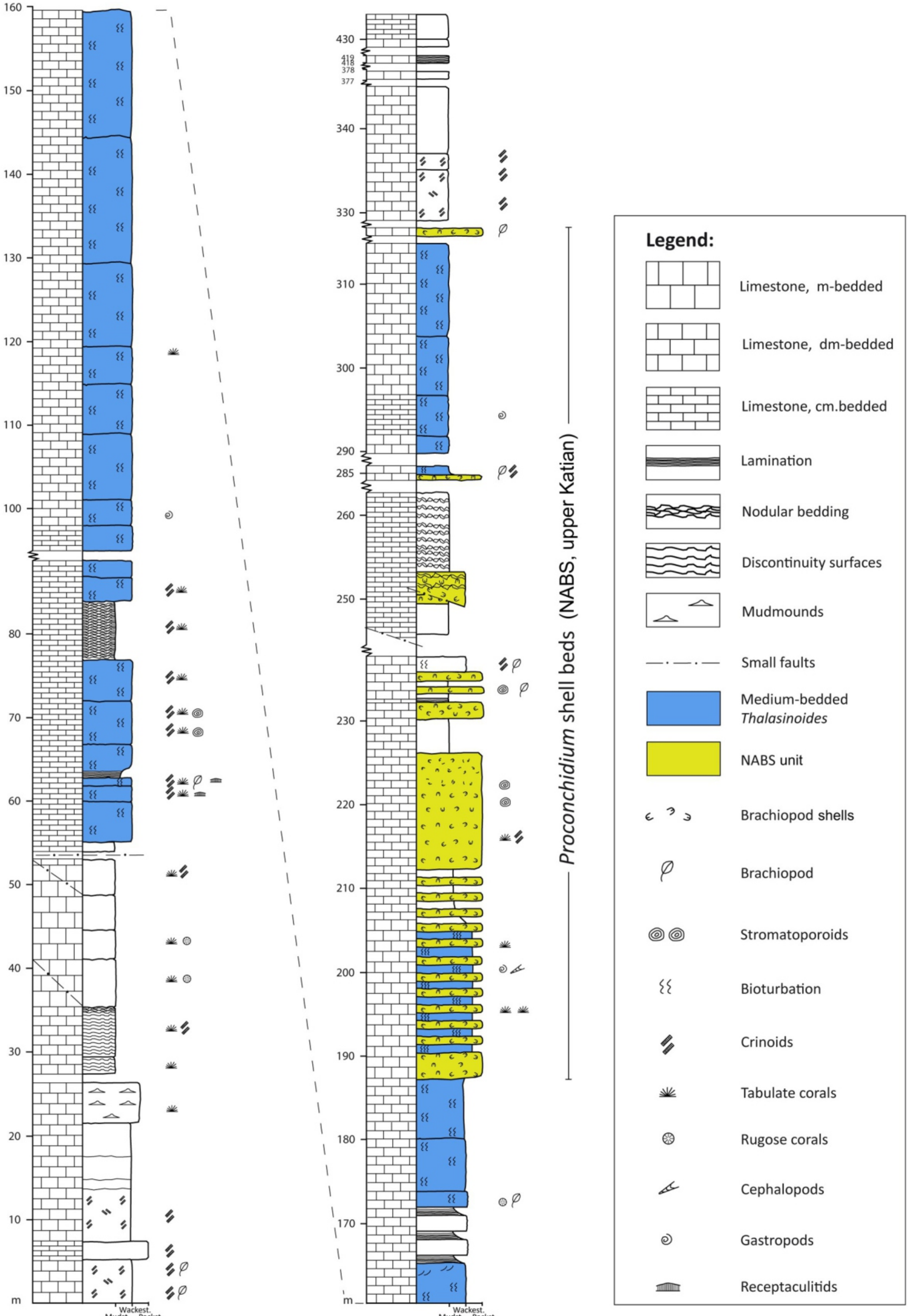

Fig. DR2 (Jin et al.)

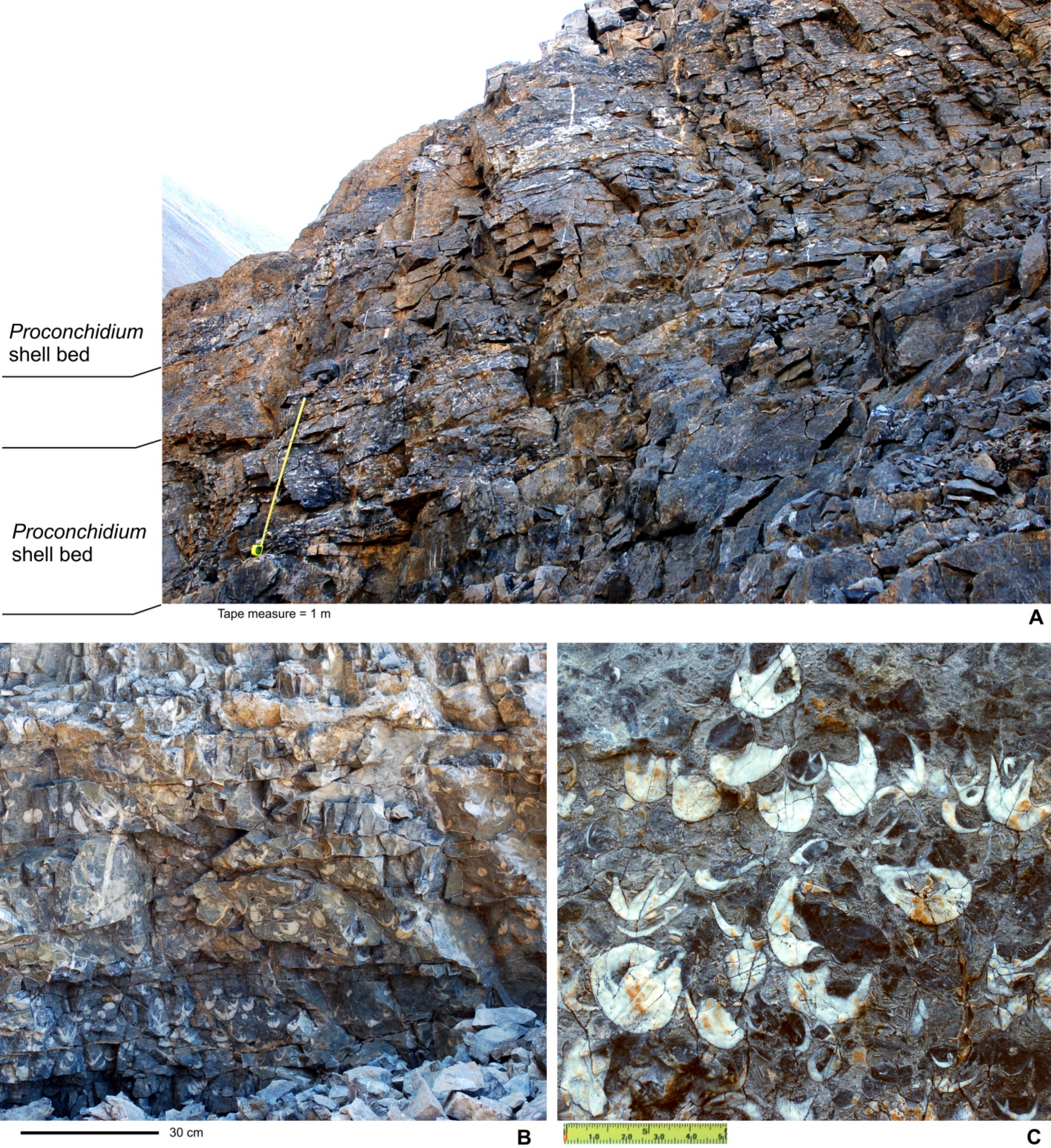

Fig. DR3 (Jin et al.)

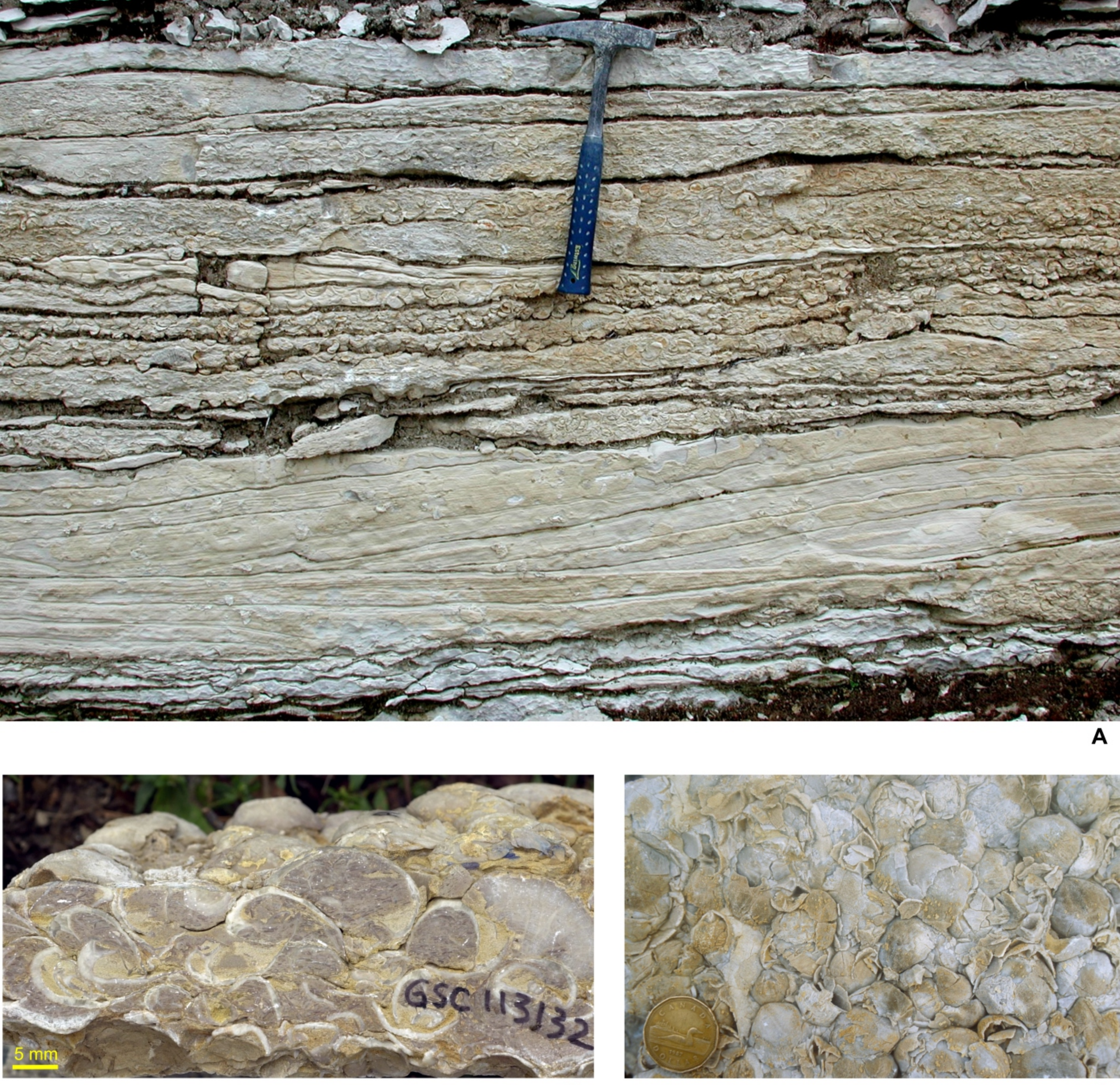

Fig. DR4 (Jin et al.)

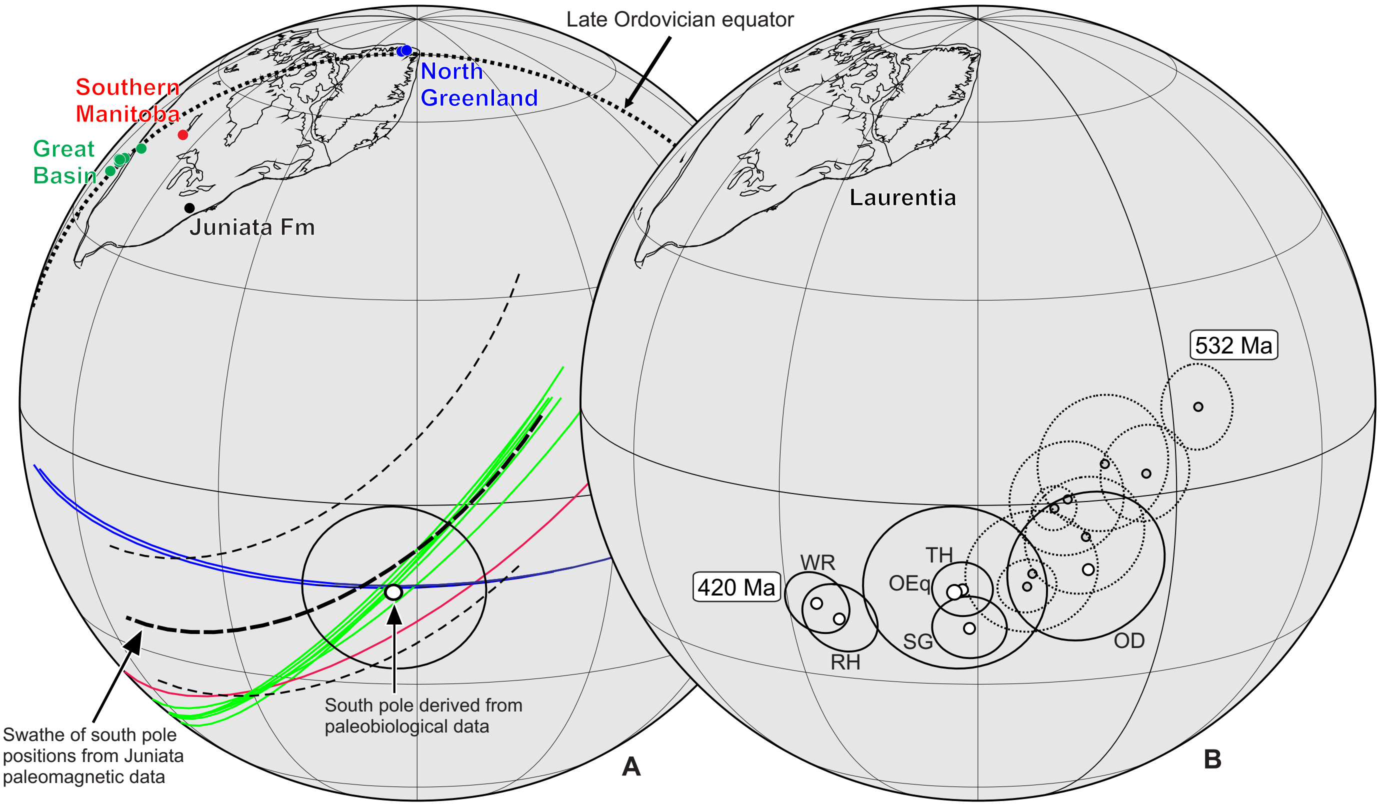

Fig. DR5 (Jin et al.)

Supplementary Table DR1. Ordovician and Silurian paleomagnetic results and south paleopole positions for Laurentia.

Code	**Rock unit, location**	**Unit age**		**Location**		**N**	**Palaeomagnetic result**			**Palaeopole (south)**			***Q***	**REFNO**
		Stratigraphic	**(Ma)**	**EN**	**E**	**sites**	***D***	***I*E**	**α_{95}E**	**EN**	**E**	**A_{95}E**	**(7)**	
WR	Wabash Reef, IN	Upper Silurian	420	40.6	274.2	12	147.1	44.2	5.1	-16.8	304.9	5.1	7	1277
RH	Rose Hill Fm., MD, WV	Middle Silurian	425	39.5	280.5	9	330.6	-44.2	5.8	-19.1	308.3	5.8	6	1218
RG	Ringgold Gap, GA	Ordovician-Silurian	~438	34.2	274.7	11	138.5	26.1	7.3	-27.9	321.4	5.8	4	1689
OEq	Late Ordovician fauna	Richmondian	445	-	-	9	-	-	-	-13.5	326.5	13.5	-	This study*
JN-s	Juniata Fm., S limb, PA	Richmondian	445	40.1	281.5	5	333.0	-43.0	18.1	-20.2	307.5	17.7	4	2295
JN-n	Juniata Fm., N limb, PA	Richmondian	445	40.5	282.7	6	357.4	-47.8	10.2	-20.6	285.1	10.7	4	2295
TH	Table Head Gp., NFLD	Darriwilian	465	48.7	301.2	13	151.6	41.7	4.4	-13.0	327.7	4.2	5	2257,1931
SG	St. George Gp., NFLD	Tremadoc-Floian	480	48.6	301.0	13	152.6	32.3	5.4	-19.5	328.7	4.6	4	1928
OD	Oneota dolomite, IL-MN	Tremadocian	480	44.0	268.0	10	105.4	2.0	11.9	-10.4	346.4	8.4	6	1283